Dalton Transactions

ROYAL SOCIETY OF CHEMISTRY

COMMUNICATION

View Article Online
View Journal | View Issue

Cite this: *Dalton Trans.*, 2020, **49**, 7304

Received 12th April 2020,
Accepted 4th May 2020

DOI: 10.1039/d0dt01340d

rsc.li/dalton

Self-assembly of mixed-valence and heterometallic metallocycles: efficient catalysts for the oxidation of alcohols to aldehydes in ambient air†

Ya-Liang Lai, Xue-Zhi Wang, Rui-Rong Dai, Yong-Liang Huang, Xian-Chao Zhou, Xiao-Ping Zhou * and Dan Li

Two mixed-valence Cu^{II}/Cu^{I} and two heterometallic Cu^{II}/Ag^{I} metallocycles have been synthesized by the assembly of designed metalloligands and Cu^{I}/Ag^{I} ions, respectively. The Cu^{II}/Cu^{I} metallocycle can catalyze the oxidation of alcohols to aldehydes mediated by a co-catalyst, TEMPO (2,2,6,6-tetramethylpiperdine-1-oxyl), with ambient air as an oxidant, while the Cu^{II}/Ag^{I} metallocycle has no catalytic effect.

The design and construction of discrete supramolecular coordination complexes (SCCs) including metallocycles and coordination cages through coordination driven self-assembly have attracted great attention due to their aesthetically pleasing structures and advanced functions (*e.g.* host–guest chemistry,[1,2] catalysis,[3,4] optical materials,[5–7] and bioengineering[8]). Metallocycles are large metal–organic rings in which metal ions bind with organic ligands through dative bonds. Due to the highly directional and relatively strong dative bonds, metallocycles can be designed and prepared with predictable shapes and sizes. A huge number of metallocycles have been successfully synthesized with various geometries (*e.g.* triangles, squares or rectangles, pentagons, hexagons, heptagons, and octagons).[9–11] In these metallocycles, the electronic state and coordination geometry of metal ions may play critical roles in both structures and functions. A metallocycle with mixed-valence or heterometallic metal ions is important,[3] as the different metal centers can probably act either as structural nodes or as functional sites. However, the self-assembly of metallocycles featuring an identical structure with mixed-valence and heterometallic metal ions is unusual, in which a precisely designed building unit is required for them to bind with different types of metal ions.

A complex that has appended functional binding sites to coordinate to additional metal ions is regarded as a metalloligand. Metalloligands have been employed in the self-assembly of metallocycles *via* a stepwise synthesis,[12,13] which is documented as a useful approach, especially for heterometallic metallocycles.[3] In our previous studies, we found that a mononuclear metal complex based on a bis-imidazole ligand with Schiff base groups can act as a metalloligand (Scheme 1 and Fig. S1, ESI†), which has been employed as a building unit to construct coordination cages and coordination polymers.[14,15] We hypothesized that this metalloligand can be probably used as a building unit for metallocycles: (1) the mononuclear metal complex contains two convergent nonbinding sites (<N–Cu–N ≈ 98°, Fig. S1, ESI†); (2) the soft nitrogen in the imidazole ligand can bind with soft linear coordinated coin metal ions (*e.g.* Cu^{I} and Ag^{I}); (3) previous reports have shown that the imidazole ligand can form metallocycles with coin metal ions.[10] Herein, we report the stepwise construction of two mixed-valence Cu^{II}/Cu^{I} and two heterometallic Cu^{II}/Ag^{I} metallocycles by using two copper(II)-imidazolate complexes as metalloligands (Scheme 1). Both the mixed-valence and heterometallic metallocycles have identical triangular structures. Interestingly, we found that the Cu^{II}/Cu^{I} metallocycle shows excellent catalytic activity for the oxidation of alcohol mediated by TEMPO, whereas there is no catalytic effect from the heterometallic Cu^{II}/Ag^{I} metallocycle. Furthermore, the Cu^{II}/Cu^{I}

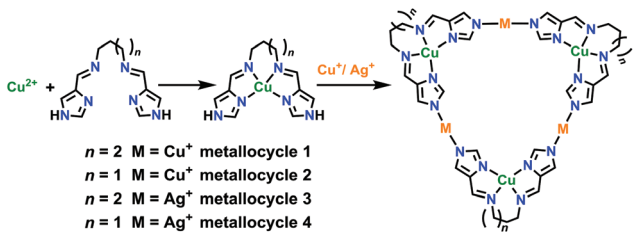

Scheme 1 Schematic representation of stepwise synthesis of metallocycles **1–4**.

College of Chemistry and Materials Science, Jinan University, Guangzhou, Guangdong 510632, P. R. China. E-mail: zhouxp@jnu.edu.cn

†Electronic supplementary information (ESI) available: Experimental section, characterization and physical measurements. CCDC No. 1963369, 1963370, 1974814 and 1974815. For ESI and crystallographic data in CIF or other electronic format see DOI: 10.1039/D0DT01340D

metallocycle can be further used to catalyze the Knoevenagel condensation of benzaldehyde and malononitrile to achieve a sequential catalysis.

Ligands H_2L1 (*N*,*N*′-(butane-1,4-diyl)bis(1-(1H-imidazol-4-yl) methanimine) and H_2L2 (*N*,*N*′-(propane-1,3-diyl)bis(1-(1*H*-imidazol-4-yl)methanimine)) were synthesized from the condensation of 4-formylimidazole with the corresponding diamine molecules (1,4-diaminobutane for H_2L1 and 1,3-diaminopropane for H_2L2).[14] Then, the mononuclear complexes $Cu(H_2L1)$ and $Cu(H_2L2)$ were obtained by reacting H_2L1 and H_2L2 with $Cu(ClO_4)_2{\cdot}6H_2O$, respectively. Finally, the metalloligands ($Cu(H_2L1)$ and $Cu(H_2L2)$) upon reacting with $Cu_2O/AgNO_3$ in mixed solvents (*N*,*N*′-dimethylacetamide (DMA)/ethanol, 2 : 1, v/v) at 100 °C for 72 h afforded four metallocycles (see the ESI† for details), formulated as $Cu^{I}_3(Cu^{II}L1)_3{\cdot}3ClO_4$ (**1**), $Cu^{I}_3(Cu^{II}L2)_3{\cdot}3ClO_4$ (**2**), $Ag^{I}_3(Cu^{II}L1)_3{\cdot}3NO_3$ (**3**), and $Ag^{I}_3(Cu^{II}L2)_3{\cdot}3NO_3$ (**4**), respectively. Single crystals of metallocycles **1–4** were obtained by solvothermal processes. Further studies found that metallocycles **1–4** can also be synthesized in one step by mixing the ligands and metal salts under similar conditions (Scheme S1, see the ESI† for details).

Single-crystal X-ray diffraction (SCXRD) analysis revealed that all the crystals of metallocycles **1–4** crystalize in the $P\bar{1}$ space group, featuring similar hexanuclear triangular structures (Fig. 1). The structure of metallocycle **1** will be described in detail as an example. Due to the low symmetry, the asymmetric unit of **1** contains one triangular metallocycle composed of 6 copper centres and 3 ligands and three ClO_4^- anions to balance the positive charges (Fig S2, ESI†). As shown in Fig. 1a, there are two types of copper centers in **1**. The first one probably has an oxidation state of +2, where Cu^{II} was chelated by ligand L1 to form a copper(II)-imidazolate metalloligand. The second one should have an oxidation state of +1, where Cu^{I} links the metalloligands to form a triangular metallocycle. The two Cu^{II} centers adopt a five-coordinated (four nitrogen atoms from the ligand, one oxygen from ClO_4^-) square pyramidal geometry and one Cu^{II} adopts a four-coordinated square planar geometry (four nitrogen atoms from the ligand), while Cu^{I} adopts a linear coordination geometry (<N–Cu–N, 171.788–175.313°). The Cu^{II}–N bond distances are in the range of 1.976–2.026 Å, while the Cu^{II}–O bond distances are obviously longer (2.452–2.524 Å) due to the Jahn–Teller effect of the copper centers. The Cu^{II}–N bond distances are longer than the Cu^{I}–N bond distances (1.857–1.868 Å), which is in good agreement with the reported mixed-valence Cu^{II}/Cu^{I} complexes.[16,17] L1 coordinates with one Cu^{II} ion and two Cu^{I} ions in **1**, bridging the metal centers to construct metallocycle **1**. The $Cu^{II}\cdots Cu^{II}$ distances in metallocycle **1** are 11.594, 11.678, and 11.724 Å, respectively, while those of $Cu^{I}\cdots Cu^{I}$ are 7.687, 8.021, and 8.181 Å, respectively. The cavity of metallocycle **1** is occupied by a ClO_4^- anion (Fig. 2a), as the guest. Due to the ClO_4^- anion binding with Cu^{II}, an inter-threading supramolecular dimer is formed, as shown in Fig. 2b. Although metallocycles with a triangular structure have been reported previously, to the best of our knowledge, the assembly of two metallocycles by threading to form a supramolecular dimer is observed for the first time.

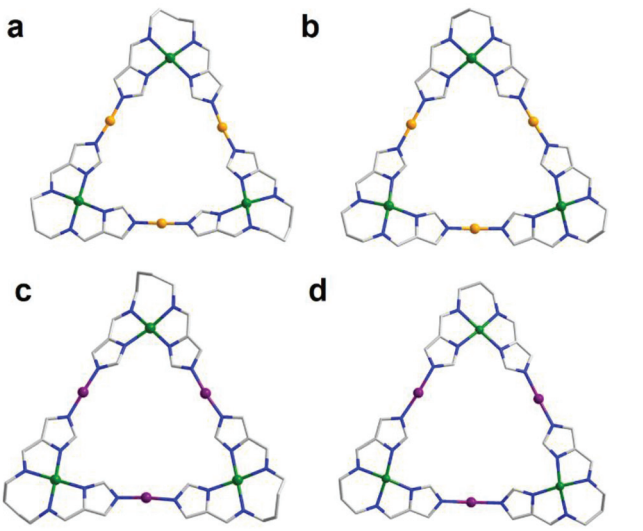

Fig. 1 Crystal structures of metallocycles **1** (a), **2** (b), **3** (c), and **4** (d). Color codes: Cu^{II}, green; Cu^{I}, orange; Ag^{I}, purple; C, light gray; N, blue. All hydrogen atoms and anions are omitted for clarity.

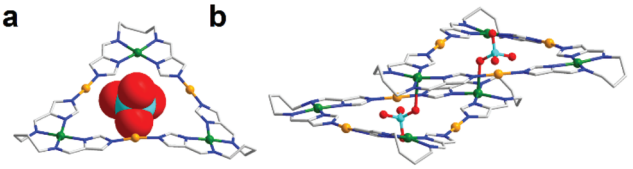

Fig. 2 Crystal structure of metallocycle **1** filled with ClO_4^- anions (a) and the structure of the inter-threading supramolecular dimer (b). Color codes: Cu^{II}, green; Cu^{I}, orange; C, light gray; N, blue; O, red; Cl, turquoise; H, omitted.

The structure of metallocycle **2** is similar to that of **1**, in which L1 is replaced with L2. The $Cu^{II}\cdots Cu^{II}$ distances (11.519–11.605 Å) in metallocycle **2** were slightly shorter than those in **1** (11.594–11.724 Å), while its $Cu^{I}\cdots Cu^{I}$ distances (8.167–8.230 Å) were slightly longer than those in **1** (7.687–8.181 Å). Upon replacing the Cu^{I} centre with Ag^{I}, similar metallocycles **3** and **4** were obtained (Fig. 1c and d), respectively. However, the $Cu^{II}\cdots Cu^{II}$ distances in both **3** (11.961–12.177 Å) and **4** (11.870–12.068 Å) were longer than those in **1** and **2**, which was probably due to their longer Ag–N coordination bond distances (2.060–2.116 Å). Interestingly, both metallocycles **3** and **4** selectively host NO_3^- anions as the guest (Fig. S3, ESI†), although the same amount of ClO_4^- anions is also present in the reaction mixture.

Powder X-ray diffraction (PXRD) analysis showed that the PXRD patterns of metallocycles **1–4** closely matched their simulated ones from the SCXRD data, indicating that the pure phase of these metallacycles can be obtained (Fig. 3a, b and Fig. S4, ESI†). To confirm the mixed-valence state of the copper centers in metallocycles **1** and **2**, the X-ray photoelectron spectra (XPS) of **1** and **2** were measured. As shown in Fig. 3c and d, intense asymmetrical Cu $2p_{3/2}$ photoelectron

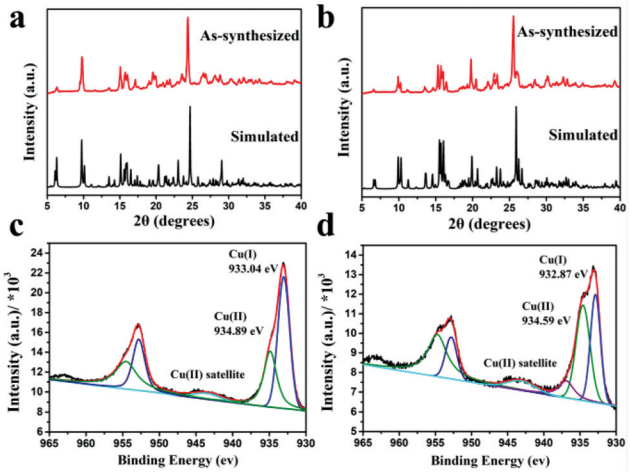

Fig. 3 PXRD patterns of **1** (a) and **2** (b) and the XPS spectra of **1** (c) and **2** (d) with fitted peaks (blue Cu^{I}; green Cu^{II}).

peaks with satellite peaks are observed in both spectra, indicating the mixed-valence feature of the copper centers in **1** and **2**.[18,19] The Cu $2p_{3/2}$ peaks can be deconvoluted into two contributions located at 933.04 and 934.89 eV for **1** (Fig. 2c) and 932.87 and 934.59 eV for **2** (Fig. 2d), corresponding to the Cu^{I} and Cu^{II} species at peak area ratios of approximately 3 : 2 and 2 : 3, respectively. The peak area ratios of Cu^{I} and Cu^{II} in the XPS are not in agreement with the crystal structures. The possible reason is that the XPS is surface-sensitive quantitative technology. On the other hand, the bond valence sum (BVS) has been used to determine the oxidation state of the metal ions based on their metal–ligand bond distances in the SCXRD structure or extended X-ray absorption fine structure (EXAFS).[20] The calculation of BVS values for the three Cu^{II} centers in **1** gives 2.037, 2.043, and 2.031, respectively, while that for the three Cu^{I} centers gives 0.981, 0.964, and 0.958, respectively. Similarly, the BVS values of the three Cu^{II} centers in **2** are 2.068, 2.105, and 2.088, respectively, while those of the three Cu^{I} centers are 0.978, 0.976, and 0.990, respectively. All these BVS values are in good agreement with the results of SCXRD and XPS, proving the mixed-valence properties of both metallocycles **1** and **2**.

Mass spectrometry was usually employed for analyzing the solution states of cages and metallocycles. The high-resolution mass spectra of metallocycles **1–4** were measured by using an electrospray ionization time-of-flight mass spectrometer (ESI-TOF-MS) in acetonitrile. As shown in Fig. S5 (ESI†), the main cationic peaks arise mainly from the broken species of the metallocycles (*e.g.* $[CuL1-H]^{+}$ and $[Cu_3L_2-4H]^{+}$ in the spectrum of **1**), indicating that metallocycles **1–4** are probably not stable during the ESI-TOF-MS measurements. However, we can observe some weak cationic peaks arising from the loss of anions and hydrogen from the metallocycles (such as *m*/*z* 603.395, $[Cu_3(CuL1)_3(ClO_4)-6H]^{2+}$ for **1**, 582.695, $[Cu_3(Cu_3L2)_3(ClO_4)-6H]^{2+}$ for **2**, 620.594, $[Ag_3(CuL1)_3\text{-}7H]^{2+}$ for **3**, and 630.530, $[Ag_3(CuL2)_3(NO_3)-6H]^{2+}$ for **4**) in the spectra, suggesting that metallocycles **1–4** should exist in acetonitrile solution.

Aldehydes play an important role in organic reactions and high-value components in the perfume industry. They can be produced from the oxidation of alcohols by employing stoichiometric amounts of inorganic oxidizing reagents, including chromium and manganese oxides.[21] Such oxidation reactions are poorly selective and generate copious amounts of heavy-metal waste, and are not environmentally friendly. Therefore, the development of green catalysts for the oxidation of alcohols by using green oxidizing reagents (*e.g.* O_2) seems highly desirable and is fundamentally important in laboratory and industrial settings.[22] The galactose oxidase (GO) enzyme containing copper catalytic centres can selectively oxidize primary alcohols to aldehydes. To mimic the GO enzyme, copper(I/II) complexes have been employed for catalysing the oxidation of alcohols to aldehydes by combining them with stable nitroxyl radicals such as TEMPO and molecular oxygen.[23–25] We hypothesize that the Cu^{II}/Cu^{I} mixed-valence metallocycles can probably act as an efficient catalyst for the aerobic oxidation of alcohols to aldehydes by using TEMPO as a co-catalyst.

The solubility of metallocycle **1** is better than that of **2** in acetonitrile. Thus, the catalytic activity of **1** for the oxidization of alcohol was assessed, and the oxidation of benzyl alcohol was selected as a model reaction. The gas chromatography (GC) results demonstrated that the oxidation of benzyl alcohol to benzyl aldehyde is successful by using metallocycle **1**, TEMPO, *N*-methylimidazole (NMI), and acetonitrile at room temperature in ambient air, in which TEMPO and NMI act as co-catalyst and base, respectively. After the optimization of the reaction parameters, the catalyst system employed here consists of 5 mol% **1**, 10 mol% TEMPO, and 50 mol% NMI in acetonitrile. As shown in Fig. S6 (ESI†), although the reaction rate is slow in the first 40 min, metallocycle **1** could catalyse the oxidation of benzyl alcohol with 99.99% conversion in 2 hours. The further oxidation of benzyl aldehyde to benzoic acid is not observed during the reaction even with longer reaction time, indicating the excellent selectivity of the catalyst. For comparison, the catalytic performance of metallocycle **3** was also assessed under the same conditions. The experimental results showed that trace benzyl aldehyde was detected, indicating that **3** cannot catalyse the oxidation of benzyl alcohol to benzyl aldehyde. The structural difference between **1** and **3** is the linear coordination of the metal ions (Cu^{I} **1**, Ag^{I} **3**), suggesting that the catalytic site in **1** is likely the Cu^{I} centre, rather than Cu^{II}. The possible reason is that Cu^{II} in both **1** and **3** is chelated by L1, which does not have an accessible active site to catalyse benzyl alcohol. Therefore, as proposed by Stahl., *et al.*,[23] the plausible mechanism may contain two important separate half-reactions (Fig. S7†). First, the O_2 of air oxidizes Cu^{I} and TEMPOH. Second, the yielded intermediate Cu^{II} species oxidize the alcohol to aldyhyde, which is mediated by TEMPO.

Inspired by the good catalytic performance of metallocycle **1** for the oxidation of benzyl alcohol to benzyl aldehyde under ambient conditions, the scope of this oxidation reaction was

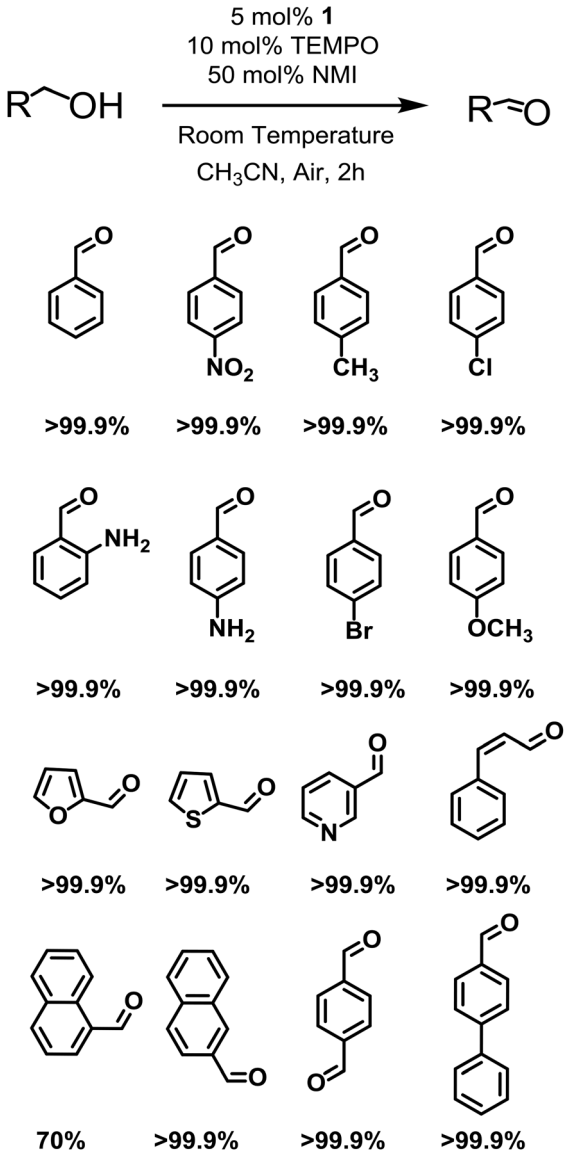

Fig. 4 The oxidation of various aromatic alcohols by metallocycle **1**.

further explored. As shown in Fig. 4, 16 aromatic alcohol molecules with various substitutional groups and heteroaromatic alcohols were tested. Both electro-withdrawing and -donating substitutional groups on the benzene ring of benzyl alcohols were well-tolerated (conversion >99.9%). On the other hand, heteroaromatic alcohols including 2-furylmethanol, 2-thienylmethanol, and 3-pyridinylmethanol also afford excellent conversion (>99.9%) in 2 h. However, for 1-naphthalenemethanol, the conversion (~70%) is obviously lower than that of 2-naphthalenemethanol, which is probably due to its steric hindrance.

As metallocycle **1** also contains weak base groups (*e.g.* imidazole and Schiff base groups), it can probably catalyze the Knoevenagel condensation reaction.[26] Thus, the sequential alcohol oxidation/Knoevenagel condensation reaction can probably be achieved by employing **1** as a catalyst (Scheme S2, ESI†). Upon the completion of oxidation of benzyl alcohol, malononitrile (2.0 equiv.) was added to the reaction mixture. The product benzylidenemalononitrile was acquired with 90.0% conversion after 1.5 h. The sequential reaction afforded an extremely low conversion (<2%) without adding **1** as a catalyst. This preliminary result showed that metallocycle **1** can be used as a potential catalyst for sequential reactions.

In summary, we have successfully constructed two mixed-valence Cu^{II}/Cu^{I} and two heterometallic Cu^{II}/Ag^{I} metallocycles by using a metalloligand approach. These metallocycles feature similar triangular structures. Interestingly, interthreading supramolecular dimers were observed between two adjacent metallocycles with their binding anions. Metallocycle **1** is an efficient catalyst for the oxidation of aromatic alcohols to aldehydes. Furthermore, metallocycle **1** can catalyze the Knoevenagel condensation reaction, providing a potential material for sequential catalysis. This work provides a good strategy for designing mixed-valence and heterometallic metallocycles. It can be expected that these interesting metallocycles can be employed as a catalyst for more organic reactions.

Conflicts of interest

There are no conflicts to declare.

Acknowledgements

This work was supported by the National Natural Science Foundation of China (no. 21731002, 21871172, and 21801095), the Major Program of Guangdong Basic and Applied Research (no. 2019B030302009), the Fundamental Research Funds for the Central Universities (21619405), and Jinan University.

Notes and references

1 F. J. Rizzuto, L. K. S. von Krbek and J. R. Nitschke, *Nat. Rev. Chem.*, 2019, **3**, 204–222.
2 X. Zhang, X. Dong, W. Lu, D. Luo, X.-W. Zhu, X. Li, X.-P. Zhou and D. Li, *J. Am. Chem. Soc.*, 2019, **141**, 11621–11627.
3 W.-X. Gao, H.-N. Zhang and G.-X. Jin, *Coord. Chem. Rev.*, 2019, **386**, 69–84.
4 J. Wei, L. Zhao, C. He, S. Zheng, J. N. H. Reek and C. Duan, *J. Am. Chem. Soc.*, 2019, **141**, 12707–12716.
5 W. Xuan, M. Zhang, Y. Liu, Z. Chen and Y. Cui, *J. Am. Chem. Soc.*, 2012, **134**, 6904–6907.
6 M. L. Saha, X. Yan and P. J. Stang, *Acc. Chem. Res.*, 2016, **49**, 2527–2539.
7 J.-P. Lang, Q.-F. Xu, Z.-N. Chen and B. F. Abrahams, *J. Am. Chem. Soc.*, 2003, **125**, 12682–12683.
8 H. Sepehrpour, W. Fu, Y. Sun and P. J. Stang, *J. Am. Chem. Soc.*, 2019, **141**, 14005–14020.
9 S. Leininger, B. Olenyuk and P. J. Stang, *Chem. Rev.*, 2000, **100**, 853–908.

10 X.-C. Huang, J.-P. Zhang and X.-M. Chen, *J. Am. Chem. Soc.*, 2004, **126**, 13218–13219.
11 T. Zhang, L. P. Zhou, X. Q. Guo, L. X. Cai and Q. F. Sun, *Nat. Commun.*, 2017, **8**, 15898.
12 W.-H. Zhang, Z.-G. Ren and J.-P. Lang, *Chem. Soc. Rev.*, 2016, **45**, 4995–5019.
13 X.-T. Qiu, R. Yao, W.-F. Zhou, M.-D. Liu, Q. Liu, Y.-L. Song, D. J. Young, W.-H. Zhang and J.-P. Lang, *Chem. Commun.*, 2018, **54**, 4168–4171.
14 X.-Z. Wang, M.-Y. Sun, J. Zheng, D. Luo, L. Qi, X.-P. Zhou and D. Li, *Dalton Trans.*, 2019, **48**, 17713–17717.
15 Y.-L. Hou, Y. Pi, X.-P. Zhou and D. Li, *Inorg. Chem.*, 2018, **57**, 2377–2380.
16 W.-X. Ni, M. Li, X.-P. Zhou, Z. Li, X.-C. Huang and D. Li, *Chem. Commun.*, 2007, 3479–3481.
17 X.-C. Huang, J.-P. Zhang, Y.-Y. Lin, X.-L. Yu and X.-M. Chen, *Chem. Commun.*, 2004, 1100–1101.
18 D. C. Frost, A. Ishitani and C. A. McDowell, *Mol. Phys.*, 1972, **24**, 861–877.
19 S. Zhang and L. Zhao, *Nat. Commun.*, 2019, **10**, 4848.
20 H. H. Thorp, *Inorg. Chem.*, 1992, **31**, 1585–1588.
21 G.-J. t. Brink, I. W. C. E. Arends and R. A. Sheldon, *Science*, 2000, **287**, 1636–1639.
22 Y.-Z. Chen, Z. U. Wang, H. Wang, J. Lu, S.-H. Yu and H.-L. Jiang, *J. Am. Chem. Soc.*, 2017, **139**, 2035–2044.
23 J. M. Hoover, B. L. Ryland and S. S. Stahl, *J. Am. Chem. Soc.*, 2013, **135**, 2357–2367.
24 J. M. Hoover and S. S. Stahl, *J. Am. Chem. Soc.*, 2011, **133**, 16901–16910.
25 J. M. Hoover, J. E. Steves and S. S. Stahl, *Nat. Protoc.*, 2012, **7**, 1161–1166.
26 Y. Y. Li, T.-Y. He, R.-R. Dai, Y.-L. Huang, X.-P. Zhou, T. Chen and D. Li, *Chem. – Asian J.*, 2019, **14**, 3682–3687.